A Novel Adaptive Approach to Fingerprint Enhancement Filter Design

A. M. Tahmasebi and S. Kasaei

Department of Computer Engineering, Sharif University of Technology, Azadi St., Tehran, Iran, P.O.Box: 11365-9517

Abstract

A novel procedure for fingerprint enhancement filter design is described. Fingerprints are best used as unique and invariant identifiers of individuals. Identification of fingerprint images is based on matching the features obtained from a query image against those stored in a database. Poor quality of fingerprint images makes serious problems in the performance of subsequent matching process. The main contribution of this work is to quantify and justify the functional relationship between image features and filter parameters. In this work, the enhancement process is adapted to the input image characteristics to improve its efficiency. Experimental results show the superiority of the proposed enhancement algorithm compared to the best fingerprint enhancement procedures reported in the literature.

Key words: biometrics identification, directional filtering, enhancement, ridge distance estimation, filter design.

1 Introduction

Fingerprint matching is the most popular biometrics technique used in automatic personal identification systems. The first application of fingerprints was in the field of criminal investigation, but nowadays with the progress in computer technology it has become more popular in different fields such as: employee identification, physical access control, and information system security. There are other biometrics techniques available such as: hand geometry, iris recognition, speakerface recognition and so forth. The main reason for popularity of fingerprint–based approaches is that each fingerprint of a person is unique and remains invariant with age. Existence of huge fingerprint databases and the fact that these

Email address: amtm@ieee.org, skasaei@sharif.edu (A. M. Tahmasebi and S. Kasaei).
URL: http://sharif.edu/∼skasaei (A. M. Tahmasebi and S. Kasaei).

are the only identifiers that remain in the scene, make the fingerprint–based identification approaches even more of interest. The accuracy of fingerprint identificationauthentication methods relies on the reliability of its features. The features used in matching can be divided into two main groups; high–level features and low–level features. By high–level features, the query fingerprint is classified into one of the five main groups (making database search to narrow down into a smaller space). The most popular high–level groups include: arch, tented–arch, left loop, right loop and whorl. The more complicated part of identification process involves in the use of low–level features, called minutiae. Minutiae (or Galton's characteristics [1]), are local discontinuities in fingerprint patterns [2]. There are 18 types of minutiae reported in the literature [3], but the most four popular features are: ridge bifurcation, ridge ending, short ridge, and ridge crossover. For automatic feature extraction and matching purposes the set of fingerprint features is restricted to two types of minutiae; ridge bifurcation and ridge ending. These are shown in figure 1.

One of the main problems in extracting structural features is due to the presence of noise. Commonly captured fingerprint images (based on inked impressions) suffer from the following types of noise: I) over–inked areas; creating smudgy areas, II)under–inked areas; creating breaks in ridges, and III) skin being elastic in nature; changing the positional characteristics of fingerprint features [4]. The aim of this work is to adapt the filter design to different input image characteristics.

Several approaches to automatic minutiae extraction have been proposed in the literature; using different types of enhancement approaches. *O'Gorman* and *Nickerson* [5] present a technique for enhancement based on convolution of image with a filter oriented according to the ridge dominant direction. *Sherlock* et al. [6,7] define a technique for fingerprint enhancement and binarization that performs a frequency domain filtering through position–dependent filters [2]. The most recent works reported in the literature [7,4], are based on the usage of Gabor filters. *C.J. Lee* and *S.D. Wang* in [7] proposed a Gabor–filter–based method for fingerprint recognition. *Jain* et al. in [4] present a fast fingerprint enhancement algorithm by the use of Gabor filters. The performance of these approaches is discussed in Section 3.

In this work an efficient and robust algorithm for a fast fingerprint enhancement process is presented. Algorithmic and quantitative details of the proposed are given in Section 2. The experimental results are discussed in Section 3, followed by the conclusion statement.

2 Proposed Fingerprint Enhancement Algorithm

This work aims at introducing a filter design procedure for fingerprint enhancement purposes which adapts itself to the characteristics of input images, with no need to use any predetermined parameters. We design an enhancement filter to increase the contrast between foreground ridges and background, and also to reduce noise in smudgy regions. To achieve this, the query image is first normalized to have zero mean and unit variance.

The main purpose of normalization is to have input images with similar characteristics and also to reduce the variation in gray–level values along the ridges and valleys (without changing the ridge and valley structures). The image is then divided into non overlapping blocks and dominant ridge directions are determined for each block [1,8], to be used in the subsequent processes. It is worth mentioning that as in this stage the only available data is the input raw image, only a coarse estimate of ridge directions can be computed, but the design of the algorithm is such that even with a coarse estimate of ridge directions the proposed enhancement process can perform properly. The dominant ridge directions are then smoothed using the method presented in [8] and subsequently the block–direction image is formed. The next step is to estimate the average ridge distance. It is also worth mentioning that as the average ridge distance of a fingerprint taken from a child, a laboring man, and a woman are different, by computing the average ridge distance the algorithm becomes scale invariant. This helps the proposed algorithm to perform properly for different people with different ages and also for different live-scan sensors with various spatial resolutions. The proposed estimation method is introduced in detail next. In this work, unlike in [4] that the ridge frequency is computed for each block of the image, in order to reduce the computational cost, in the proposed algorithm the average ridge distance is computed once for the whole input image. This parameter is then used to determine the block size as well as the filter mask size. Knowing the size of the mask, other proposed filter parameters can now be determined. The image is then enhanced using the directional filtering method. In summary to enhance the query image:

(1) normalize the query image,
(2) compute the local ridge orientations,
(3) smooth the obtained directions,
(4) estimate the average ridge distance,
(5) determine the proposed filter parameters, and
(6) implement directional filtering to enhance the image.

The details of each stage are given next.

2.1 Block–Direction Image

In this work the dominant ridge directions in each $N \times N$ block is given as [1]:

$$\theta_b = \frac{90}{\pi} tan^{-1} \frac{\Sigma_{m=1}^{N} \Sigma_{n=1}^{N} 2G_x(m,n)G_y(m,n)}{\Sigma_{m=1}^{N} \Sigma_{n=1}^{N} [G_x^2(m,n) - G_y^2(m,n)]} \quad (1)$$

where G_x and G_y are the gradient magnitudes obtained using 3×3 sobel masks. To get the correct θ_b between 0 to 180 degrees, (as stated in [8]) we first check the signs of the numerator and denominator. If denominator is positive we add 90 to θ_b, if denominator is negative and nominator is positive we add 180 to θ_b, and otherwise θ_b is unchanged.

Since the block–direction image is computed from the raw input image (which is noisy), smoothing process of directional image is inevitable. As the enhancement process is dependent to the accuracy of the directional image, any improvements in the quality of directional image will directly affect the performance of enhancement process. To smooth the directional image we use the method presented by *S. Kasaei* et al. in [8].

2.2 Estimation of Average Ridge Distance

In the fingertip pattern the distance between adjacent ridges (valleys) is almost constant. In the proposed filter coefficients' assignment procedure some of the parameters, especially the filter mask size, are directly related to the value of average ridge distance. In this section the proposed average ridge distance estimation process is presented. In the first step in order to compute a correct average ridge distance value a search is done all over the block–direction image to find a region having the least variance in direction sense, and hence to find a "clear" foreground area. According to the search result, the determined block and its nine neighboring blocks are selected to be used in the process (as shown in figure 2). Based on the corresponding direction the summation along the ridge dominant direction is computed to specify the ridge start points. The mean of the obtained distances is then assigned as the average ridge distance of the image. The algorithm is as follows:

$$
\begin{aligned}
&\text{for } i = 1 : 3 \times \text{blksize} \\
&\qquad x_i = i; \\
&\qquad y_i = tan\theta_b(x_i - x_s) + y_s; \\
&\qquad round(y_i); \\
&\\
&x_j = 3 \times \text{blksize}; \\
&\text{for } j = 1 : 3 \times \text{blkisize} \\
&\qquad y_j = tan\theta_b(x_j - x_s) + y_s; \\
&\qquad round(y_j);
\end{aligned}
\tag{2}
$$

where (x, y)s are the coordinates of the ridge points and (x_s, y_s)s are the start points of the ridges included in the block resulting from the summation and average process of the previous step and $blksize$ is the block size.

2.3 Filter Mask Design

In this section, the proposed filter design process is described. Before presenting the closed–form equation of the filter and its parameter determination, filter characteristic have to be specified. The following criteria should be met by the filter:

(1) The filter should improve the clarity between ridge and valley structures. It should be done in a way that the middle of ridge areas be weighted at most and the middle of valley areas be weighted at least; while it does not change the natural shape of the fingerprint pattern.
(2) The filter mask should be symmetric about its axis (of orientation).
(3) Performance of the filter should be independent to image scale.
(4) In order to meet the admissibility condition, the filter should be zero biased (to obtain block gray–level intensity invariant condition).

A matched filter is the most suitable choice to meet the above criteria. Here, a filter bank is considered (containing masks with different sizes where the size depends on the amount of the average ridge distance). As it will be stated in the following sections, the filter mask has a closed–form equation; and therefore determination of filter parameters is adequate to obtain different masks. In the reminder of this section we refer to the filter mask which is oriented horizontally. The rows of the mask are perpendicular to the ridge direction while the columns are parallel to the ridge orientations. Here, the row indices are denoted by i. The value of i is zero in the center, negative to the left and positive to the right. Column indices are denoted by j. The value of j is zero in the center, negative above and positive below the center. The closed–form of the filter is given by:

$$f(i,j) = [w_1 exp(-\alpha i^2) - \ w_2 exp(-\beta(i-\tau)^2) \\ - w_2 exp(-\beta(i+\tau)^2)] \tag{3}$$

where w_1 and w_2 characterize the weights given to the middle of ridge and valley areas, respectively. These values in fact directly affect the DC value of the filter mask. α and β specify the sharpness and roughness of the filter, respectively (and hence they are directly related to the ridge distance). The last parameter τ, is used to meet the symmetric conditions of the filter and its value depends on the ridge distance as well. The mask size is determined by the average ridge distance, λ, such that to contain one period of the signal, *e.g.*:

$$\text{masksize} = \begin{cases} \lambda + 2, & \text{for odd } \lambda \\ \lambda + 1, & \text{otherwise.} \end{cases} \tag{4}$$

Figure 3 shows the 3–D shape of the proposed filter.

Other filter orientations are formed by rotating the horizontally oriented mask to the desired angle. The coefficients at location (i', j') on the rotated mask are found by rotating the angle back to its original location (i, j):

$$\begin{bmatrix} i' \\ j' \end{bmatrix} = \begin{bmatrix} \cos\theta & \sin\theta \\ -\sin\theta & \cos\theta \end{bmatrix} \begin{bmatrix} i \\ j \end{bmatrix}. \tag{5}$$

Usually the (i, j) locations will not fall exactly on the sampling location. When this happens, the coefficients of the rotated mask at (i', j') are calculated as a function of four coefficients of the original mask nearest to (i, j) by Lagrangian interpolation. These four coefficient coordinates are denoted as $(i_L, j_L), (i_L, j_U), (i_U, j_L), and (i_U, j_U)$ with subscripts L and U denoting the lower and upper sampling locations nearest to (i, j). Then [5]:

$$\begin{aligned} f(i', j') = &(j_U - j')(i_U - i')f(i_L, j_L) \\ &+(i' - i_L)(j_U - j')f(i_U, j_L) \\ &+(j' - j_L)(i_U - i')f(i_L, j_U) \\ &+(j' - j_L)(i' - i_L)f(i_U, j_U). \end{aligned} \tag{6}$$

2.4 Enhancement

After calculating the filter parameters for different mask sizes and preparing a library of horizontally oriented filters, now we can implement the enhancement operations. First, the query image is extended in each side by $e = \text{round}(\frac{1}{\sqrt{2}} \times \lambda)$ to avoid artificial grid lines causes by convolution with a rotated filter and also to consider the ridge energy in neighboring blocks to maintain ridge continuities. For each $(N + e) \times (N + e)$ overlapping block, the horizontally oriented filter is rotated according to the smoothed dominant ridge direction and convolved with the block. The middle $(N \times N)$ enhanced blocks is then replaced to its original location. The process then continues for the whole image. Figure 4 shows a block of image before and after implementing the proposed enhancement process.

3 Experimental Results

Using 512×512 fingerprint images with 256 gray–levels (500 dpi), the enhancement process starts with normalization of the input images; to have zero mean and unit variance. The dominant ridge directions are then computed and smoothed using the algorithm stated in [8]. For filter mask designation process, the size of the filter mask is computed using the proposed average ridge distance estimation method described in Section 2.2. For instance for ridge distance $\lambda = 10$, the mask size is 11×11 and the filter parameters in equation

(2) are: $w_1 = 1, w_2 = .5, \alpha = 10, \beta = 10, \text{and} \tau = e - 1$, where $e = round(\frac{1}{\sqrt{2}} \times \lambda)$. To enhance the image, each block is extended by e(*e.g.* 2×5 for $\lambda = 10$) number of pixels in each direction. The designed filter is rotated according to the obtained smoothed dominant ridge direction of that block. The rotated filter is then convolved with that block to form the enhanced block. Figure 5 shows the result of the enhancement process using the proposed algorithm as well as the best two other approaches stated in the literature [4,5]. We have tested the performance of the proposed enhancement algorithm on about 150 fingerprint images (taken from [9]). To show the efficiency of the proposed enhancement algorithm we have used 22 typical fingerprint and have applied the proposed as well as [4] and [5] algorithms on them. We have used the *Group Goodness Scale* criteria to quantitatively assess the performance of different algorithms. The overall goodness criterion rates image quality on scale ranging from Best to Worst (as shown in Table 1). Table 2 shows the result of the subjective test run on these images. According to 22 observers' grades given for different algorithms, the mean rating, R, is calculated for each method as:

$$R = \frac{\Sigma_{k=1}^{n} s_k n_k}{\Sigma_{k=1}^{n} n_k} \tag{7}$$

where s_k is the score associated with the kth rating, n_k is the number of observers with this rating, and n is the number of grades in the scale. Mean ratings obtained for the proposed, [4] and [5] algorithms are 5.66, 5.40, and 1.62, respectively. The performance of the enhancement process can also be judged by applying the subsequent ridge extraction and thinning algorithms and comparing the quality of obtained thinned images as well as the reliability of extracted minutiae. Figure 6 illustrates the thinned images obtained from different enhancement approaches. Tables 3 reports the results of different methods, when applied on a set of eight typical fingerprint images, in terms of dropped (undetected), false (non-existent), and exchanged minutiae. Table 4 lists the average error percentage of a sample set containing 150 typical fingerprint images.

4 Conclusion

A novel and efficient procedure for an adaptive fingerprint enhancement filter design is proposed. To improve the efficiency of the enhancement process, the designed filter adapts itself to the characteristics of input images. Moreover, the filter parameters are automatically calculated with no need of any predetermined parameters. Different filter masks are adapted for different image scales to improve the efficiency of the enhancement process. The algorithm is fast and the required computational load is negligible. Experimental results clearly show the superiority of the proposed algorithm compared with the best enhancement approached stated in the literature.

References

[1] F. Galton, Fingerprints, (London: Macmillan, 1982).

[2] D. Maio, Direct Gray–Scale Minutiae Detection in Fingerprints, *IEEE Trans. on Pattern Analysis and Machine Intelligence*,**19** (1) (January 1997) 27–40.

[3] Federal Bureau of Investigation(FBI),The Science of Fingerprints: Classification and Uses, (U.S. Government Printing Office, Washington, D.C., 1984).

[4] A. Jain, L. Hong and Y. Wan, Fingerprint Image Enhancement Algorithm and Performance Evaluation, *IEEE Trans. on Pattern Analysis and Machine Intelligence* **20** (8) (August 1998) 777–789.

[5] L. O'Gorman and J. V. Nickerson, An Approach to Fingerprint Filter Design, *Pattern Recognition*, **22** (1) (1989) 29–38.

[6] B. G. Sherlock, D. M. Monro, and K. Millard, Algorithm for Enhancing Fingerprint Images, *Electronics Letters* **28** (18) (1992) 1920–1921.

[7] C. J. Lee and S. D. Wang, A Gabor Filter–Based Approach to Fingerprint Recognition, *IEEE Workshop on Signal Processing System, SiPS 99.*, (1999) 371–378.

[8] S. Kasaei et al., Fingerprint Feature Extraction using Block–Direction on Reconstructed Images, *Region 10 Annual Conference, Speech and Image Technologies for Computing and Telecommunications, Proceedings of IEEE* **1** (1997) 303–306, and also *http://mehr.sharif.edu/∼siprl/pub/icics02.pdf.*

[9] C. I. Watson and C. L. Wilson, Fingerprint Database, *National Institute of Standards and Technology (NIST)*, (August 1995).

List of Captions:

Fig. 1: Two commonly used fingerprint features:
(a) ridge bifurcation, (b) ridge ending.

Fig. 2: Illustration of proposed average ridge distance estimation algorithm.

Fig. 3: 3–D shape of proposed enhancement filter.

Fig. 4: (a) original block, (b) enhanced block.

Fig. 5: Performance comparison of different enhancement algorithms:
(a) original image, (b) proposed algorithm, (c) algorithm stated in [5], (d) algorithm stated in [4].

Fig. 6: Performance analysis of different enhancement algorithms after applying the ridge extraction and thinning processes:
(a) original block, (b) proposed algorithm, (c) algorithm stated in [5], (d) algorithm stated in [4].

Table 1: Group Goodness Scales.

Table 2: Result of subjective test run on 22 typical fingerprint images.**A** and **B** denote the methods presented in [5] and [4], respectively. Each column denotes the frequency of allocated grades.

Table 3: Statistical analysis of extracted minutiae obtained from different algorithms. [Column 1: input figure number, Column 2: minutiae type, Column 3: total number of grand truth minutiae, **d**, **f** and **x** denote the number of dropped, false, and exchanged minutiae, respectively. Also **A** and **B** denote the methods presented in [5] and [4], respectively.]

Table 4: Average Error percentage obtained from 150 typical fingerprint images.

List of Figures and Tables:

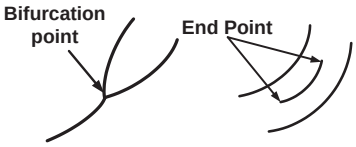

(a) (b)

Fig. 1.

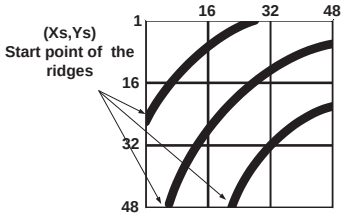

Fig. 2.

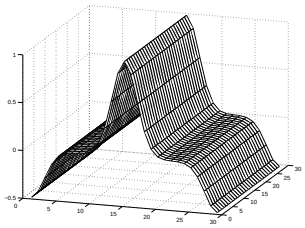

Fig. 3.

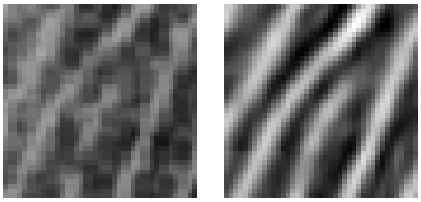

(a) (b)

Fig. 4.

(a) (b)

(c) (d)

Fig. 5.

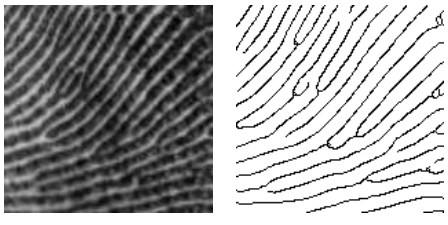

(a) (b)

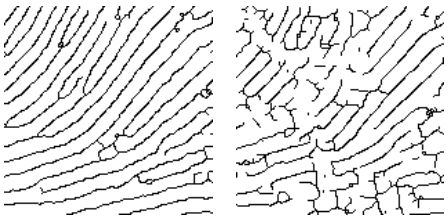

(c) (d)

Fig. 6.

Table 1

Grade	Group Goodness Scale
7	Best
6	Well above average
5	Slightly above average
4	Average
3	Slightly below average
2	Well below average
1	Worst

Table 2

Grade	Proposed	A [5]	B [4]
7	61	45	0
6	120	102	0
5	94	104	0
4	26	43	3
3	7	14	39
2	0	0	105
1	0	0	161

Table 3

N	F	T	A			B [5]			C [4]		
			d	*f*	*x*	*d*	*f*	*x*	*d*	*f*	*x*
1	**B**	10	-	1	3	2	-	4	11	12	7
	E	15	6	-	1	4	-	1	8	17	9
2	**B**	23	1	1	1	4	-	3	7	13	8
	E	34	2	-	5	5	1	6	9	17	5
3	**B**	29	4	-	2	5	1	2	7	15	4
	E	25	3	1	5	7	1	5	10	12	7
4	**B**	22	1	1	2	5	2	2	5	9	5
	E	51	2	-	1	6	1	2	12	9	7
5	**B**	26	4	-	8	3	-	9	9	10	6
	E	35	6	-	3	10	-	4	14	12	5
6	**B**	24	2	-	5	10	-	5	10	9	4
	E	28	2	1	1	10	1	2	8	14	7
7	**B**	35	3	1	5	8	1	10	7	8	4
	E	19	2	-	3	1	-	4	4	6	6
8	**B**	24	4	-	3	6	-	5	7	10	7
	E	31	2	1	2	4	-	4	5	14	9

Table 4

Err. Type	Proposed	A [5]	B [4]
Dropped	10.20%	20.88%	30.86%
False	01.62%	01.86%	43.39%
Exchange	11.60%	15.78%	23.20%
Total Err.	23.42%	38.52%	97.45%